

# Positronium time-of-flight Measurements of Mesoporous Silica Films<sup>‡</sup>

PENG KUANG<sup>a</sup>, XIAOWEI ZHANG<sup>b</sup>, CHUNQING HE<sup>b</sup>, XINGZHONG CAO<sup>a</sup>, AND BAOYI WANG<sup>a,\*</sup>

<sup>a</sup>Institute of High Energy Physics, Chinese Academy of Sciences, Beijing 100049, China

<sup>b</sup>School of Physics and Technology, Wuhan University, Wuhan 430072, China

Mesoporous silica films were synthesized with various concentrations of cetyltrimethylammonium bromide (CTAB) in precursor sols through the method of electro-assisted self-assembly (EASA). Oriented pore channels were observed in the films prepared with more CTAB in the precursor sols. Positronium time-of-flight (Ps-TOF) measurements were performed for the silica films with different porous structures. It is demonstrated that the Ps emission intensity and energies are well correlated to the apparent porosity, pore interconnectivity and possibly pore channel orientation. The results indicate that Ps-TOF can be a useful technique for probing the structures of porous films.

DOI: [10.12693/APhysPolA.133.3](https://doi.org/10.12693/APhysPolA.133.3)

PACS/topics: 78.70.Bj; 61.05-a; 68.47.Mn

## 1. Introduction

In recent years, many efforts have been devoted to promote directed assembly of mesophases because tunable orientation of the mesoporous network is highly required for numerous applications [1–3]. Electrochemistry is likely to induce self-assembly of cetyltrimethylammonium bromide (CTAB)-templated silica thin films on various conducting supports, with mesoporous channels oriented perpendicular to the solid surface over wide areas [4]. A major factor for the optimization of pore characteristics is the selection of a suitable sol solution.

The influence of the CTAB/TEOS concentration ratio on the mesoporous structure has not been thoroughly examined [5]. Slow positron annihilation spectroscopy is a powerful tool to study the in-depth variation of membrane fine structure [6–8]. In this paper, we report a study of positronium time-of-flight (Ps-TOF) spectra using variable energy monoenergetic slow positron beams to study the positron annihilation characterization in mesoporous silica films (200 nm) formed with three different CTAB/TEOS ratios electrodeposited on a very flat indium tin oxide (ITO) substrate.

Positronium (Ps), a bound state of an electron and a positron [9], is a unique atom whose total spin can be easily derived by analyzing its self-annihilation mode. For example, ortho-Ps (o-Ps) is the triplet state Ps with total spin  $S = 1$ . Ps-TOF is a technique for measuring the energy of o-Ps in flight, which used for studying fundamental issues related to Ps emission from the surfaces of materials [10]. Energetic Ps formed within a mesopore (2–50 nm scale pore) undergoes millions of collisions with the pore wall before it escapes from the sample by finding a route through an open channel to the surface [11].

Hence the energy of emitted o-Ps provides information on the open pore characteristics of silica films [12, 13].

## 2. Experiment

### 2.1. Ps-TOF experiments

Measurements were conducted with a newly developed TOF system in combination with an intense slow positron beam. About  $10^6$  slow positrons/s are generated with a 50 mCi  $^{22}\text{Na}$  radiation source and accelerated by a negative high voltage applied to the samples. The beam was bunched into 2 ns wide pulses at a frequency of 100 Hz. As shown in Fig. 1, four plastic scintillators placed symmetrically at  $360^\circ$  in a plane behind a lead slit of 3 mm width detected  $\gamma$  rays from the o-Ps decay at distance  $z$  from the sample surface. The TOF spectra were recorded on a multi-channel analyzer using a time to amplitude converter with a start signal supplied by the signal of the buncher of pulsing system and the stop signal by the  $\gamma$  ray signal detected by one of the four plastic scintillators.

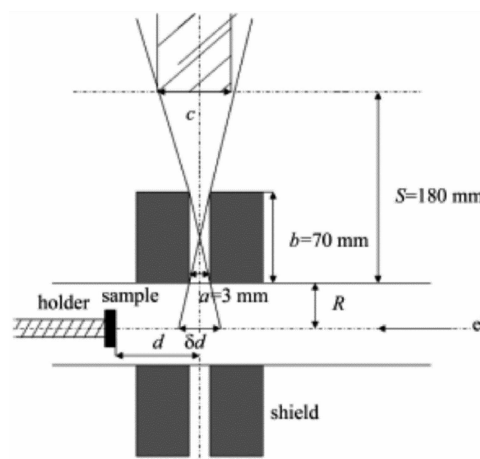


Fig. 1. Diagram of TOF system:  $c = 13$  mm,  $R = 30$  mm,  $\delta d = 5.6$  mm,  $-20$  mm  $\leq d \leq 80$  mm.

\*corresponding author; e-mail: [wangboy@ihep.ac.cn](mailto:wangboy@ihep.ac.cn)

<sup>‡</sup>delayed submission to Vol. 132, November issue.

## 2.2. Sample preparation

Tetraethoxysilane (TEOS, 98%, Alfa Aesar), ethanol (95-96%, Merck),  $\text{NaNO}_3$  (99%, Fluka), HCl (37%, Riedel de Haen) and cetyltrimethylammonium bromide (CTAB or C16TAB, 99%, Acros) were used as received for film synthesis. Electro-assisted deposition [4, 14] of mesoporous silica thin films on indium-tin oxide (ITO) glass was achieved using ITO (surface resistivity) 8–12  $\Omega$ , Delta Technologies) and Pt electrodes. A typical sol consisted of 40 mL of ethanol, 40 mL of an aqueous solution of 0.1 M  $\text{NaNO}_3$ , to which were added 50–340  $\text{mmol L}^{-1}$  TEOS and 12–544  $\text{mmol L}^{-1}$  CTAB surfactant under stirring. HCl was added in order to make the pH of the sols to close 3. The resultant precursor sols, composed of a water/ethanol mixture (50:50 volume ratio), TEOS and CTAB with various CTAB/TEOS molar ratios, were stirred for 2.5 hours at room temperature. During electro-assisted deposition, the Pt electrode and a saturated calomel electrode were used as the counter and reference electrodes, respectively, and the ITO cathode potential was biased to  $-1.3$  V for 120 s. After deposition, the films were washed several times using ethanol in order to remove residual chemicals in the porous structures. The final films, synthesized using precursor sols with CTAB/TEOS molar ratios of 0.08, 0.16 and 0.32, were denoted as film (a), (b) and (c), respectively.

## 3. Results and discussion

### 3.1. Porous structure of silica films

Transmission electron microscopy was used to investigate the microstructures of the obtained silica films and the images are shown in Fig. 2. Various porous structures are observed for the three films prepared with different CTAB/TEOS ratios. As shown in Fig. 2A, plenty of “isolated” pores with disordered structure can be seen for film (a). While, from Fig. 2B and 2C, well-ordered pore channels are found for films (b) and (c), which were synthesized with more CTAB template. Simultaneously, the pore channel orientation in film (b) was worse than that in film (c). With increasing CTAB/TEOS molar ratio to 0.32, it seems that not only the channel pore orientation but also the connectivity of pore channels is improved in film (c).

Further, apparent porosities of the prepared silica films were investigated by ellipsometry. The apparent porosity (pore volume fraction  $V_p$ ) of the silica films is estimated by Lorentz–Lorenz equation [15] which can be simplified as

$$\frac{n^2 - 1}{n^2 + 2} = (1 - V_p) \frac{n_s^2 - 1}{n_s^2 + 2}$$

where  $n$  and  $n_s$  refer to the refractive index of the porous film and silica skeleton, respectively. The refractive index of amorphous silica (1.45) is used as the value of  $n_s$  in the Lorentz–Lorenz equation. The refractive index and the porosity of the silica films as a function of CTAB/TEOS molar ratios are shown in Fig. 3. It can be seen that the

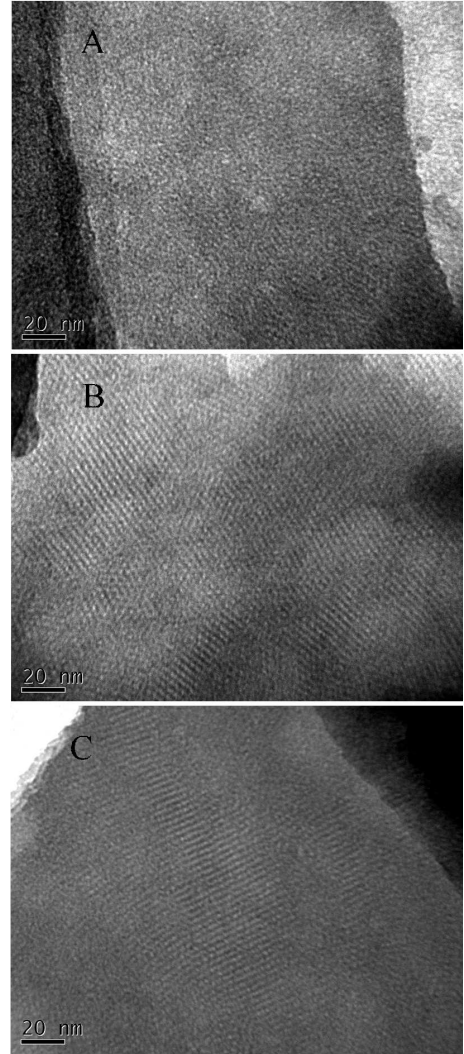


Fig. 2. TEM images for the films (a), (b) and (c).

refractive index decreases from around 1.325 to 1.15 with more CTAB due to development of porous structures. Accordingly, the apparent porosity grows monotonically from 22% to 61% with increasing CTAB/TEOS molar ratio from 0.08 to 0.32, indicating that the CATB surfactant plays an important role in the porous structures of the silica during electro-assisted deposition.

### 3.2. Ps-TOF measurement

The effects of the o-Ps intrinsic decay and time spent by o-Ps in the view of the scintillation detectors were corrected by multiplying the factor  $\exp(t/142 \text{ ns})/t$  to the as-recorded TOF spectra after subtraction of the time-independent, random background. The time scale was then converted to an energy scale based on the relation  $E = m_e(d/t)^2$ , where  $m_e$  is the electron mass and  $d$  is the o-Ps flight length. Finally, the TOF spectra were normalized. For instance, the Ps-TOF spectra for film (b) collected at different o-Ps flight lengths  $d$  (see Fig. 1)

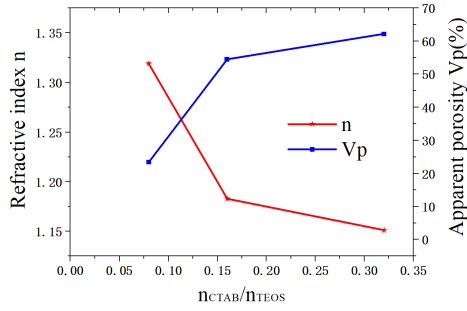


Fig. 3. Apparent porosity and refractive index of the silica films as a function of CTAB/TEOS molar ratios.

at  $E_{in} = 0.1$  keV are presented in Fig. 4. Time zero of the spectra was determined as the peak position of the intense prompt signals due to positron annihilation in the sample. With increasing Ps flight distance, the detected Ps annihilation peaks were shifted to a longer time. The validity of the Ps-TOF data is confirmed by an excellent proportionality between the TOF peak position  $T$  and the flight length  $d$ , as shown in the inset of Fig. 4.

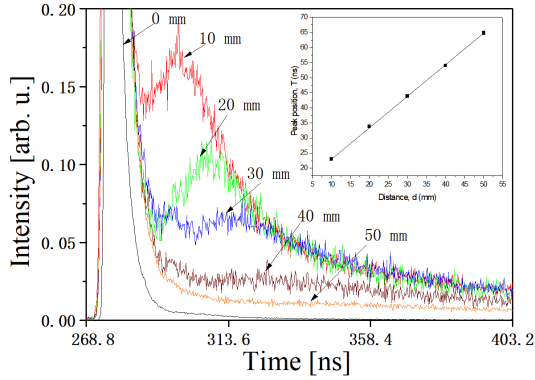


Fig. 4. Ps-TOF spectra with the positron energy of 0.1keV for the film (b) at different positions.

### 3.3. Correlation between Ps-TOF results and pore characteristics

Figure 5 shows the Ps emission energy spectra for films (b) and (c) at incident positron energies between 0.1 and 3.0 keV obtained by Ps-TOF measurements at 20 mm flight length. The prompt counts above 10 eV are due to the interference of scattered  $\gamma$ -rays produced by the positron annihilation in the sample. Clear *o*-Ps emission peaks are observed for both films (b) and (c) at an incident positron energy of 0.1 and 0.3 keV, at which positronium atoms are formed and emitted from the film sub-surfaces. With increasing  $E_{in}$ , the *o*-Ps peak intensities of film (c) are weakened and the peak positions shifted from about 3 eV to around 0.1 eV, because positronium atoms formed deeply in films have to diffuse a longer way to the surface before flying to the detecting region, and

they may annihilate and/or collide with the pore walls in a high number during diffusion. The longer diffusion length and stronger Ps-pore surface interaction can result in a reduction in the number of Ps and a lower energy of emission. Hence, information about pore interconnectivity, and possibly orientation of ordered channel pores can be correlated to Ps emission energy spectra.

However, with further increasing positron incident energy beyond 1.0keV, no intense *o*-Ps emission peak can be found for the film (b). This means that almost no *o*-Ps can escape from a deeper level region of film (b). This results seems to conflict with the fact that the apparent porosities of film (b) and (c) are essentially the same, as indicated by the ellipsometry results. Considering the TEM observation of microstructures of them, it is likely that channel pore interconnectivity is less and the orientation of pores is worse in film (b) than those in film (c) despite the observation that their apparent porosities are almost same.

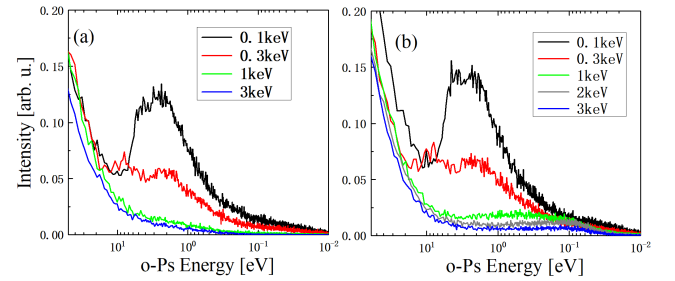


Fig. 5. Emission energy spectra of *o*-Ps for films (b) and (c) measured at a fixed *o*-Ps flight length of 20 mm. The incident positron energy varied from 0.1 keV to 3.0 keV.

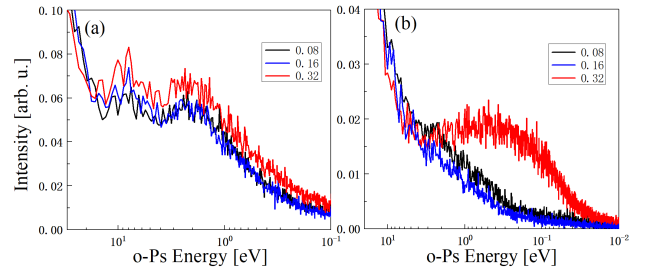


Fig. 6. Positronium emission energy spectra measured at positron incident energies (a) 0.3 keV and (b) 1 keV for the porous films with different concentrations of CTAB.

Figure 6 shows a comparison of the emission energy spectra of *o*-Ps for the films prepared with different concentrations of CTAB. As the incident positron energy  $E_{in}$  is lower than 0.3 keV, most emission Ps atoms possess kinetic energies of a few eVs, due to the emission of Ps from the subsurface. And the *o*-Ps emission intensity from surface around 5-10 eV Ps energy follows the order: film (a)<film (b)<film (c), being associated with the ap-

parent porosity  $V_p$  of the films in Fig.3, while the one around Ps energy 1.5–4 eV is not. It indicates that the emission intensity of Ps from the subsurface could not be related to the porosity of the films directly taking into account features of the porous channels. With increasing the positron incident energy, the Ps emission peak in the film (c) shifts to a lower emission energy but it still is high, revealing that high interconnectivity and much ordered pore structures exist in film (c) prepared with more CTAB. Further, when the incident positron energy is 1.0 keV, the emission intensity of Ps, from film (a) with much lower apparent porosity, is obviously higher than that from the film (b). This result strongly suggests that although ordered pores with high density are formed in film (b), the pore interconnectivity and possibly the orientation is still low. This useful information about pores in the silica films cannot be derived by TEM observation, indicative of the usefulness of Ps-TOF technique for the studies of porous films.

#### 4. Conclusions

In summary, a series of mesoporous silica films were synthesized using various ratios of CTAB in precursor sols by electro-assisted deposition. The porosity and pore structures were investigated by ellipsometry and TEM, respectively. The apparent porosity of the silica films increased with more CTAB and ordered pore channels were formed. However, Ps-TOF results indicated that the pore interconnectivity and possibly orientation of the pores may be low in the film despite the high porosity and local ordered pore structures, and that ordered pore channels with high interconnectivity and orientation can be obtained in the films with much more CTAB. The results indicate that Ps-TOF can be a useful supplementary technique for studying the microstructure of porous films.

#### References

- [1] C. Sanchez, B. Julian, P. Belleville, M. Popall, *J. Mater. Chem.* **15**, 3559 (2005).
- [2] B.J. Scott, G. Wirnsberger, G.D. Stucky, *Chem. Mater.* **13**, 3140 (2001).
- [3] M. Hartmann, *Chem. Mater.* **17**, 4577 (2005).
- [4] A. Walcarius, E. Sibottier, M. Etienne, J. Ghanbaja, *Nat. Mater.* **6**, 602 (2007).
- [5] C. Sanchez, C. Boissiere, D. Grosso, C. Laberty, L. Nicole, *Chem. Mater.* **20**, 682 (2008).
- [6] P. Sferlazzo, S. Berko, K. F. Canter, *Phys. Rev. B* **35**, 5315 (1987).
- [7] A.P. Mills, E.D. Shaw, R.J. Chichester, D.M. Zuckerman, *Phys. Rev. B* **40**, 2045 (1989).
- [8] Y. Nagashima, Y. Morinaka, T. Kurihara, Y. Nagai, T. Hyodo, T. Shidara, K. Nakahara, *Phys. Rev. B* **58**, 12676 (1998).
- [9] A. Rich, *Rev. Mod. Phys.* **53**(1), 127 (1981).
- [10] R.S. Yu, T. Ohdaira, R. Suzuki, K. Ito, K. Hirata, K. Sato, Y. Kobayashi, *Appl. Phys. Lett.* **83**, 4966 (2003).
- [11] D.W. Gidley, W.E. Frieze, T.L. Dull, A.F. Yee, E.T. Ryan, H.-M. Ho, *Phys. Rev. B* **60**, R5157 (1999).
- [12] C. He, T. Ohdaira, N. Oshima, M. Muramatsu, A. Kinomura, R. Suzuki, T. Oka, Y. Kobayashi, *Phys. Rev. B* **75**, 195404 (2007).
- [13] C. He, S. Wang, Y. Kobayashi, T. Ohdaira, R. Suzuki, *Phys. Rev. B* **86**, 075415 (2012).
- [14] A. Goux, M. Etienne, E. Aubert, C. Lecomte, J. Ghanbaja, A. Walcarius, *Chem. Mater.* **21**(4), 731 (2009).
- [15] P. Revol, D. Perret, F. Bertin, F. Fusalba, V. Rouesac, A. Chabli, G. Passemard, A. Ayrat, *J. Porous Mater.* **113**, 12 (2005).